ACS POLYMERS Au
AN OPEN ACCESS JOURNAL OF THE AMERICAN CHEMICAL SOCIETY

pubs.acs.org/polymerau
Article

Influence of Metal Identity and Complex Nuclearity in Kumada Cross-Coupling Polymerizations with a Pyridine Diimine-Based Ligand Scaffold

Published as part of ACS Polymers Au virtual special issue "2023 Rising Stars".

Andrew J. King, Jiashu Wang, Tianchang Liu, Adharsh Raghavan, Neil C. Tomson,* and Aleksandr V. Zhukhovitskiy*

Cite This: *ACS Polym. Au* 2023, 3, 475−481

ABSTRACT: Cross-coupling polymerizations have fundamentally changed the field of conjugated polymers (CPs) by expanding the scope of accessible materials. Despite the prevalence of cross-coupling in CP synthesis, almost all polymerizations rely on mononuclear Ni or Pd catalysts. Here, we report a systematic exploration of mono- and dinuclear Fe and Ni precatalysts with a pyridine diimine ligand scaffold for Kumada cross-coupling polymerization of a donor thiophene and an acceptor benzotriazole monomers. We observe that variation of the metal identity from Ni to Fe produces contrasting polymerization mechanisms, while complex nuclearity has a minimal impact on reactivity. Specifically, Fe complexes appear to catalyze step-growth Kumada polymerizations and can readily access both Csp^2−Csp^3 and Csp^2−Csp^2 cross-couplings, while Ni complexes catalyze chain-growth polymerizations and predominantly Csp^2−Csp^2 cross-couplings. Thus, our work sheds light on important design parameters for transition metal complexes used in cross-coupling polymerizations, demonstrates the viability of iron catalysis in Kumada polymerization, and opens the door to novel polymer compositions.

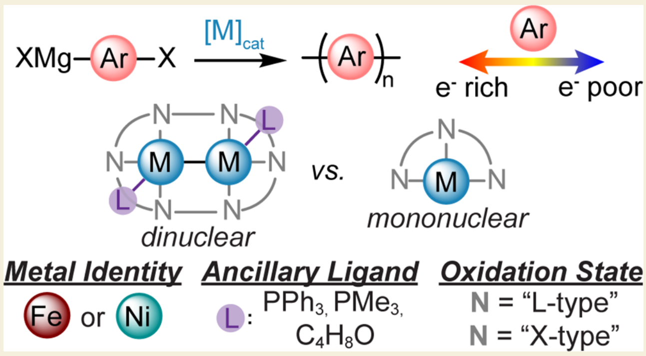

KEYWORDS: *dinuclear, transition metal, Kumada cross-coupling, polymerization, mechanism*

INTRODUCTION

Since their conception in the early 19th century, conjugated polymers (CPs) have been investigated for their unique combinations of mechanical and optoelectronic properties desirable in modern photonics, bioelectronics, and sensor applications.[1] Historically, broader utilization of CPs was accelerated by the development of cross-coupling—e.g., Kumada, Suzuki, Stille, and Negishi—polycondensation reactions, which granted access to a broader scope of CP compositions (e.g., Kumada in Figure 1A).[2] However, major drawbacks remain for the more commonly utilized methods—Suzuki, Stille, and Kumada cross-coupling, namely, boron-based substituents of the "Suzuki monomers" require multistep installations frequently accompanied by challenging purifications.[3−5] In the case of Stille cross-coupling, stoichiometric toxic tin compounds are consumed and generated.[6] Lastly, for Kumada cross-coupling, catalysts generally suffer from narrow monomer scopes.[7,8] Virtually all of these cross-coupling transformations rely on mononuclear transition metal (TM) complexes as catalysts, which limits the scope of the accessible reactivity. Alternatively, complexes with multiple metal centers can unlock new forms of reactivity and effectively expand the "toolbox" for chemical transformations—as evidenced by examples in both synthetic and biological systems.[9−12]

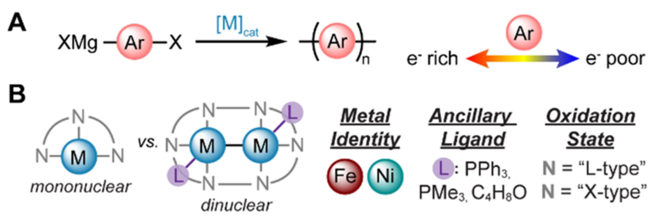

Figure 1. (A) Generic reaction scheme for Kumada cross-coupling polymerization. (B) Assortment of TM complex features explored in our investigation of Kumada cross-coupling polymerization. C_4H_8O = tetrahydrofuran.

Received: August 25, 2023
Revised: October 18, 2023
Accepted: October 20, 2023
Published: November 8, 2023

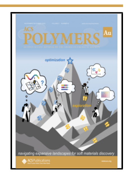

https://doi.org/10.1021/acspolymersau.3c00022
ACS Polym. Au 2023, 3, 475−481

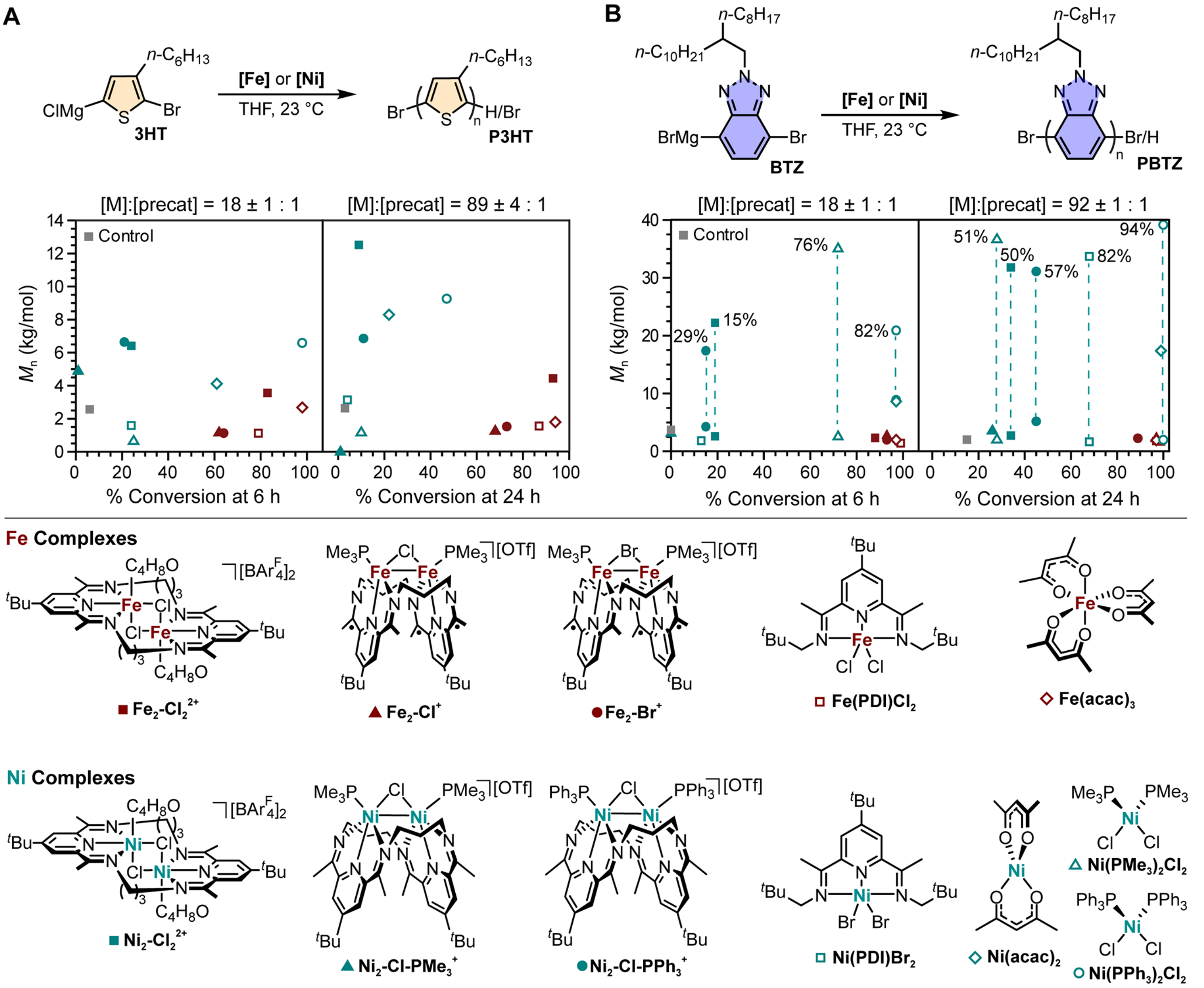

Figure 2. (A, B) Number-average molecular weights (M_n) vs % conversion for polymerizations of **3HT** (A) and **BTZ** (B). For **BTZ** polymerizations, bimodal distributions of molecular weights were observed, so the M_n-s of both modes are reported, the M_n-s are connected by a dashed line, and the % weight fraction of the higher M_n mode is given. "Control" refers to no complex being added, and [M] and [precat] refer to the concentrations of monomer and TM precatalyst.

However, to date, only a handful of examples of dinuclear complexes have been explored for CP synthesis;[13−16] moreover, numerous unknowns remain about the fundamental reactivity of dinuclear complexes in cross-coupling transformations. Additionally, while previous work has shown the influence of metal identity within a group (e.g., Ni vs Pd),[17] the influence of metal identity across a period (e.g., Ni vs Fe) has not been systematically studied in the context of cross-coupling polymerization of conjugated monomers. Thus, we sought to elucidate for a class of TM complexes with the same core ligand the broad-stroke relationships between Kumada cross-coupling polymerization reactivity and the identity, nuclearity, and oxidation state of the TM, as well as the effects of other ligands (Figure 1A,B).

Based on the findings from our previous work,[16] we sought a catalyst scaffold that (1) had a redox-active ligand, (2) placed the metals in proximity of each other, (3) formed complexes with multiple different first-row metals, and (4) could be readily compared to mononuclear analogs. We selected the bis(pyridine diimine) scaffold pioneered in the Tomson group because it fits these criteria and allowed us to investigate both nickel and iron complexes.[18−25] Notably, iron complexes are widely used for small molecule Kumada cross-coupling but, to our knowledge, had not been reported for Kumada cross-coupling polymerization.[26,27]

■ RESULTS AND DISCUSSION

With a ligand scaffold selected, we began our investigation of the reactivity of dinuclear and mononuclear Ni and Fe complexes with structurally cognate bis- and mono(pyridine diimine) ligands (Figure 2A,B, SI Table S1, and SI Figures S1−S27). As our monomers, we selected prototypical donor and acceptor ones—**3HT** and **BTZ**, respectively (Figure 2A,B)—to explore the effect of monomer electronics on the polymerization metrics: specifically, % monomer conversion and polymer (**P3HT** and **PBTZ**, Figure 2A,B) number-average molecular weight (M_n), degree of polymerization (DP), and molecular weight dispersity ($Đ$). Additionally, to provide insight into the ability to control M_n, we conducted polymerizations with both a low and a high monomer/precatalyst ratio ([M]/[precat]).

M_n versus % monomer conversion for each polymerization is plotted in Figure 2A,B (SI Tables S2, S3 and SI Figures S28–S57). Note that consumption of monomer was tracked using ^{1}H nuclear magnetic resonance (NMR) spectroscopy with an internal standard, and absolute M_n-s were determined using gel permeation chromatography (GPC) with a multiangle light scattering detector (GPC-MALS). Analysis of these data revealed several general trends. First, compared to analogous Ni complexes, both mononuclear and dinuclear Fe complexes exhibit substantially higher (in some cases, nearly complete) consumption of monomers and produce oligomers and polymers of substantially lower M_n-s. Specifically, with the exception of **Fe$_2$–Cl$_2$$^{2+}$**, the Fe precatalysts oligomerize **3HT** (M_n = 1.12–2.68 kg/mol; DP = 6–15; $Đ$ = 1.1–2.1) and **BTZ** (M_n = 1.39–2.80 kg/mol; DP = 3–7; $Đ$ = 1.3–1.6); the product identity was characterized by a combination of ^{1}H NMR spectroscopy and matrix-assisted laser desorption/ionization time-of-flight mass spectrometry (MALDI-TOF/MS) (SI Figures S58 and S59). Notably, **Fe$_2$–Cl$_2$$^{2+}$** afforded **P3HT** with M_n = 4.43 kg/mol (DP = 26; $Đ$ = 1.43) for [M]/[precat] = 93:1, which underscores the potential of Fe-based complexes in Kumada cross-coupling polymerizations. Increasing [M]/[precat] has little effect on M_n for both **3HT** and **BTZ** for all Fe complexes tested.

In contrast to Fe, the tested Ni complexes generally exhibit a lower consumption of monomer but produce polymers with much higher DPs (Figure 2B). Specifically, [18 ± 1]:[1] polymerizations of **3HT** and **BTZ** with **Ni$_2$–Cl$_2$$^{2+}$**, **Ni$_2$–Cl-PPh$_3$$^+$**, and **Ni(PPh$_3$)$_2Cl_2$** yielded **P3HT** with M_n = 6.41–6.64 kg/mol (DP = 38–39; $Đ$ = 1.3–2.2), and **PBTZ** with M_n = 17.4–22.2 kg/mol (DP = 43–55; $Đ$ = 1.3–1.5). Increasing [M]/[precat] to [89 ± 4]:[1] yields higher-DP polymers for both **3HT** (M_n = 6.84–12.5 kg/mol; DP = 40–74; $Đ$ = 1.2–1.6) and **BTZ** (M_n = 31.1–39.5 kg/mol; DP = 78–99; $Đ$ = 1.5–1.6), though the increase is lower than expected based on the change in [M]/[precat]. Notably, polymerizations of **BTZ** produced **PBTZ** characterized by bimodal distributions of molecular weights (SI Figure S43 and S44), with mononuclear Ni precatalysts producing larger weight fractions of the high-M_n species compared to dinuclear complexes. We hypothesize that the bimodal distributions are an outcome of catalyst speciation in the polymerization reactions.[28−30] Our data also revealed that both mono- and dinuclear Ni complexes with PMe$_3$ as an ancillary ligand consumed less monomer and produced lower-M_n polymers compared to those with PPh$_3$. The diminished reactivity of complexes with stronger-binding PMe$_3$ suggests that phosphine ligand dissociation may gate polymerization in those cases, particularly in the dinuclear systems.[31]

Taken together, these data paint a picture of contrasting polymerization mechanisms for Fe and Ni precatalysts. Specifically, the high conversions and low DPs in the majority of Fe-catalyzed polymerizations are suggestive of step-growth polymerization, while the low conversions and high DP for Ni-catalyzed reactions are indicative of chain-growth. The contrasting reactivity of Fe and Ni complexes is likely due to the ability of Ni complexes to suppress chain-transfer by remaining associated with a single growing polymer chain, while Fe complexes are unable to do this, which results in rampant chain-transfer and decreased M_n. In the case of the polymerization of **3HT** with **Fe$_2$–Cl$_2$$^{2+}$**, the observation of higher MW **P3HT** prompted additional kinetic investigation. Analysis of monomer consumption vs time in an 18:1 polymerization revealed an induction period of ~40 min followed by monomer consumption over the next 80 min (SI Table S4 and SI Figures S60, S61). Furthermore, M_n increases rapidly at low monomer consumption, which suggests a chain-growth mechanism is operative (SI Table S4 and SI Figures S60–S62).[32,33] Mechanistically, this suggests that the active catalyst formed in the reaction of **Fe$_2$–Cl$_2$$^{2+}$** with **3HT** is able to prevent rampant chain transfer and thereby achieve a higher MW of **P3HT**, compared to the other Fe complexes studied.

To further probe the reaction mechanisms, we conducted Kumada cross-coupling reactions of nonpolymerizable model substrates with select dinuclear and mononuclear Fe and Ni complexes that performed well in the polymerizations (**Fe$_2$–Cl$_2$$^{2+}$**, **Ni$_2$–Cl$_2$$^{2+}$**, **Fe(PDI)Cl$_2$**, and **Ni(PDI)Br$_2$**) (Table 1).

Table 1. Small Molecule Cross-Coupling with Selected Nickel and Iron Complexes

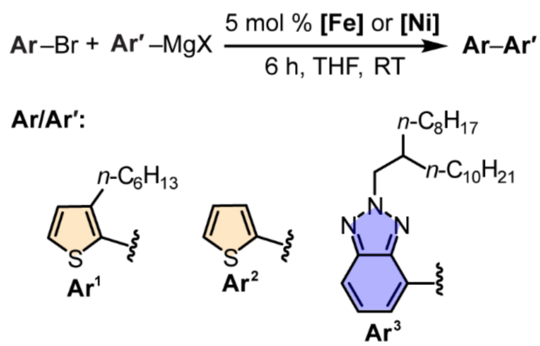

Precatalyst	Ar	Ar′	% Consumption Ar–X [a]	% Yield Ar–Ar′ [a]
Fe$_2$-Cl$_2$$^{2+}$	Ar^1	Ar^2	1	0
Fe(PDI)Cl$_2$	Ar^1	Ar^2	0	0
Ni$_2$-Cl$_2$$^{2+}$	Ar^1	Ar^2	1	0
Ni(PDI)Br$_2$	Ar^1	Ar^2	1	0
Fe$_2$-Cl$_2$$^{2+}$	Ar^3	Ar^3	26	37
Fe(PDI)Cl$_2$	Ar^3	Ar^3	35	41
Ni$_2$-Cl$_2$$^{2+}$	Ar^3	Ar^3	6	18
Ni(PDI)Br$_2$	Ar^3	Ar^3	1	12

[a]% consumption and % yields determined via ^{1}H NMR.

Cross-coupling of 2-bromo-3-methylthiophene (**Ar^1–Br**) with a thiophene Grignard (**Ar^2–MgBr**) yields stoichiometric (relative to precatalyst) amounts of the Grignard homocoupling product (**Ar^2–Ar^2**) in all cases; however, no cross-coupling product (**Ar^1–Ar^2**) analogous to the corresponding polymerizations was observed for any of the complexes under reaction conditions (SI Table S5 and SI Figure S63).

In the case of Ni complexes, we hypothesize the lack of catalytic turnover arises from kinetic competition between the productive oxidative addition reaction of Ni(0)—formed from Ni(II) after two sequential transmetalations and reductive elimination—with the aryl halide, and the off-cycle comproportionation reaction of Ni(0) and Ni(II), which generates catalytically inactive Ni(I). Support for this mechanistic proposal was gained from cyclic voltammetry (CV) experi-

https://doi.org/10.1021/acspolymersau.3c00022
ACS Polym. Au 2023, 3, 475−481

Scheme 1. Proposed Mechanisms for Chain- and Step-Growth Polymerizations/Oligomerizations of 3HT and BTZ with Mononuclear and Dinuclear Fe and Ni Complexes

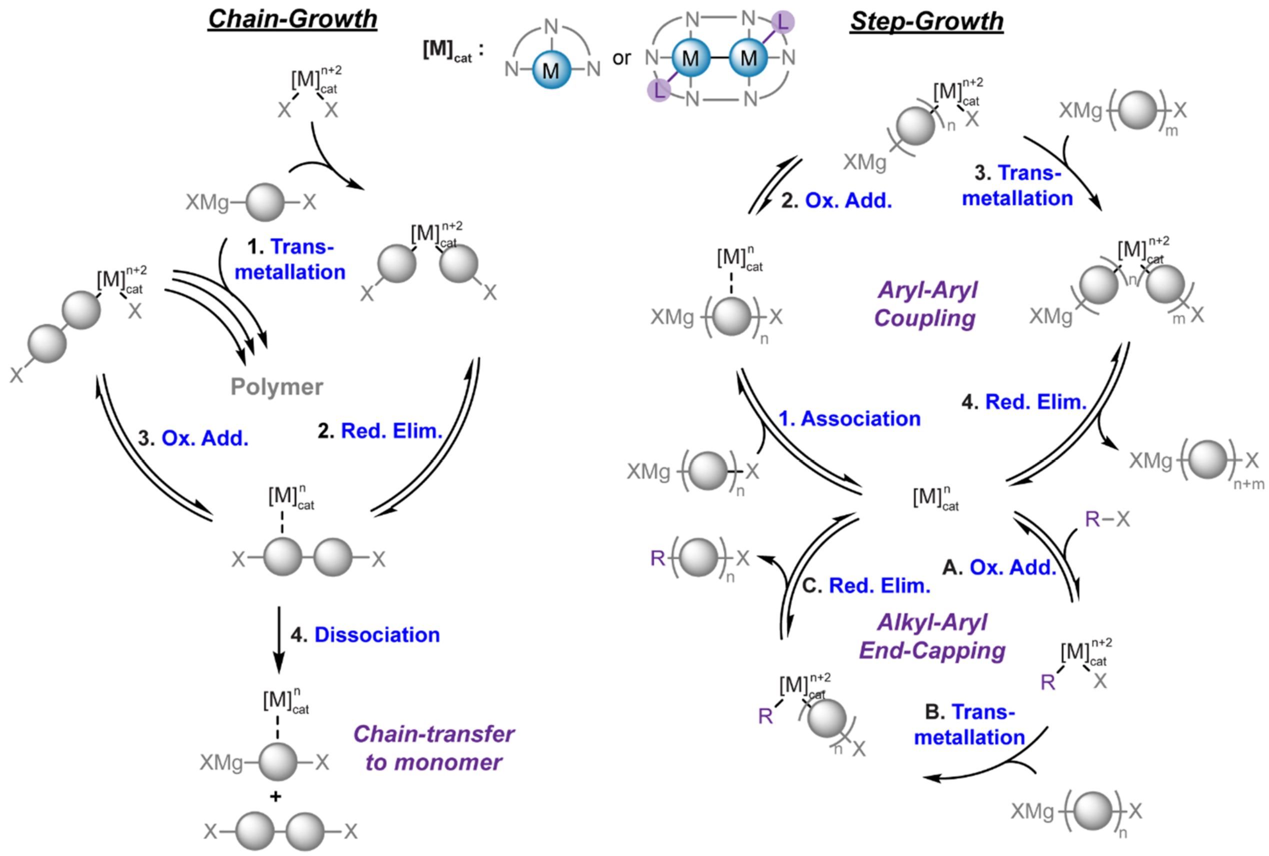

ments and stoichiometric investigations. CV of the Grignard monomers revealed irreversible oxidations at +0.1 V and −0.3 V vs Fc^+/Fc for **BTZ** and **3HT**, respectively (SI Figure S64). These reduction potentials revealed the need for more cathodic potentials to effect outersphere electron transfer with the metal complexes (SI Figures S65−68). The reduction of Ni(PDI)Br_2, for example, requires a potential of −1.6 V vs Fc^+/Fc, suggesting that either an inner-sphere electron transfer or a reductive elimination process is providing access to the active catalyst.

Treatment of **Ni(PDI)Br_2** with 1 equiv of **3HT** resulted in the formation of a mono-PDI Ni(I) bromide species, **Ni(PDI)Br**. Based on the crystallographic and X-ray absorption near edge structure (XANES) data for both this complex and **Ni(PDI)Br_2** (SI Table S1 and SI Figures S4, S69−S71), the reduction appears to be centered at Ni instead of the redox-active ligand. On treatment of **Ni(PDI)Br_2** with 1 equiv of **Ar^2**−MgBr, 2,2′-bithiophene was generated, as determined by gas chromatography mass spectroscopy (GC-MS) and NMR spectroscopic analysis (SI Figures S72−S74). These results suggest that a double ligand exchange reaction occurs in solution to yield 0.5 equiv of $Ni^{II}(PDI)(C_4H_3S)_2$, which reductively eliminates 2,2′-bithiophene and forms a Ni(0) product. This product then comproportionated with the remaining 0.5 equiv of **Ni(PDI)Br_2** to afford **Ni(PDI)Br**. To test this hypothesis, we generated a "Ni(0)" material [**Ni(PDI)**] in situ via chemical reduction of **Ni(PDI)Br_2** with 2 equiv of KC_8. This procedure resulted in a rapid color change from orange to brown. Upon treatment of this mixture with 1 equiv of **Ni(PDI)Br_2**, another rapid color change from brown to purple was observed. UV−vis and ^{1}H NMR spectroscopic analyses of the resulting mixture were consistent with the formation of **Ni(PDI)Br** (SI Figures S75 and S76), indicative of the comproportionation reaction. As expected, no reaction was observed on the treatment of **Ni(PDI)Br** with **3HT** or **BTZ** under the polymerization reaction conditions, but the treatment of **Ni(PDI)** with one equivalent of 2-bromothiophene led to gradual consumption of the aryl halide and formation of a new set of diamagnetic ^{1}H NMR features (SI Figure S77). In analogous polymerizations, these competitive reactions are not problematic for a chain-growth mechanism because the product of reductive elimination contains an aryl−halide bond, so intramolecular oxidative addition can occur rapidly before comproportionation.

For Fe-catalyzed cross-couplings, the lack of formation of **Ar^1**−**Ar^2** in the model reactions is difficult to rationalize by comproportionation side-reactions because it should affect the polymerization in the same manner due to its step-growth nature. Thus, we hypothesize that either the presence of both the Grignard and halide moieties in **3HT** activates the latter for polymerization or the presence of 2-iodopropane—a by-product of forming **3HT** but not **Ar^2**−MgBr—facilitates catalyst turnover. Analysis of the polymerization of **3HT** with **Fe_2−Cl_2^{2+}** using MALDI-TOF/MS reveals some i-Pr/Br terminated chains and confirms that 2-iodopropane is involved in the polymerization (SI Figure S58). However, when **Ar^2**−MgBr is formed analogously to **3HT**—via Grignard metathesis that generates 2-iodopropane—the outcome of the model cross-coupling reaction with **Ar^1**−Br is virtually unchanged (SI

https://doi.org/10.1021/acspolymersau.3c00022
ACS Polym. Au 2023, 3, 475−481

Table S6 and SI Figure S78). Therefore, our working hypothesis is that the presence of both Grignard and halide moieties in the substrate is the critical factor that enables aryl—aryl cross-coupling catalyzed by these Fe complexes.

For cross-coupling of benzotriazole-based small molecules **Ar^3^**—Br and **Ar^3^**—MgBr, whether dinuclear or mononuclear, the Fe and Ni complexes produce **Ar^3—Ar^3** in 37—41% and 12—18% yield, respectively (Table 1, SI Table S7, and SI Figures S79—S85). Note that we distinguish homo- and cross-coupling in this case by monitoring the consumption of **Ar^3**—Br (Table 1). Higher **Ar^3—Ar^3** yields—mostly through cross-coupling (Table 1)—for the Fe complexes in these reactions are consistent with the higher conversions observed for [18 ± 1]:[1] polymerizations of **BTZ** with the same Fe and Ni precatalysts (88—99 and 13—19%, respectively). Furthermore, in these Fe-catalyzed model reactions, we observed higher conversions of **Ar^3**—MgBr (69—81%) than **Ar^3**—Br (37—41%), which pointed to side-product formation. Indeed, ^{1}H NMR analysis of the reaction mixtures revealed formation of 4-*n*-butyl-2-(2-octyldodecyl)-2*H*-benzo[*d*][1,2,3]triazole (**4-Bu-BTZ**) in 27—31% yield, which accounts for the "excess" consumption of **Ar^3**—MgBr (SI Table S7 and SI Figures S86—S88). Fe complexes are well-known to catalyze Csp^2—Csp^3 cross-coupling, so we attributed the formation of this product to cross-coupling of **Ar^3**—MgBr with 1-bromobutane, a byproduct of **Ar^3**—MgBr formation (see SI section on "Procedure to prepare stock solution with benzotriazole Grignard"). In Ni complexes, Csp^2—Csp^3 cross-coupling was much less prominent, with at most 7% yield of **4-Bu-BTZ**. The observed Csp^2—Csp^3 cross-coupling for both Fe and Ni is expected to limit M_n-s in the polymerization reactions through "end-capping" growing chains, which is exactly what we observe for Fe (Scheme 1 and Figure 2B). Additionally, MALDI-TOF/MS for the polymerization of **BTZ** with **Fe_2—Cl_2^{2+}** reveals several chain-end combinations, including Br/Br, Br/H, *n*-Bu/Br, *n*-Bu/H, and *n*-Bu/*n*-Bu (SI Figure S59). Despite constraining the polymer molecular weights, these results represent rare examples of Csp^2—Csp^3 and Csp^2—Csp^2 Kumada cross-coupling for dinuclear complexes.

To mitigate the end-capping with 1-bromobutane, we eliminated it from our polymerization mixtures by using two equiv of *t*-BuLi for the lithium-halogen exchange step in the preparation of **BTZ**. Polymerizations with an 88:1 [M]/[precat] ratio were performed with the Fe complexes and select Ni complexes. Analysis of conversion and M_n revealed only minor differences in these metrics between reactions with and without 1-bromobutane (SI Table S8 and SI Figures S89—S91). In the case of the Ni complexes, these results are consistent with inherently low levels of Csp^2—Csp^3 cross-coupling observed in the model studies. Furthermore, the formation of high-M_n polymers at low-to-moderate conversions indicates that chain-growth polymerization is operative for both mono- and dinuclear Ni complexes (Scheme 1). In the case of Fe complexes, the inability to increase the polymer M_n despite the absence of 1-bromobutane points to another source of stoichiometric imbalance of Grignard and halide moieties, which would limit M_n in a step-growth mechanism (Scheme 1).[32] In our system, functional group imbalance results from a small amount of quenched Grignard and residual starting material as well as an initiation event that consumes two Grignard functionalities to make a biaryl species. As demonstrated in the modified Carother's equation,[34] 10% of stoichiometric imbalance is sufficient to dramatically reduce the theoretical MW for step-growth polymerizations, even at nearly quantitative conversions of the limiting reagent. Such imbalances are challenging to eliminate for a number of reasons, including an inability to purify the Grignard monomer after its formation. Thus, alternative types of monomers (e.g., aryl-zinc species) could be better suited for iron-catalyzed cross-coupling polymerizations.[35−38]

Collectively, these mechanistic investigations reveal contrasting reactivity of the Ni and Fe complexes, regardless of their nuclearity—both in their polymerization mechanisms (Scheme 1) and selectivity for Csp^2—Csp^3 vs Csp^2—Csp^2 cross-coupling. In the pyridine diimine-ligated complexes investigated here, precatalyst nuclearity has a subtle effect on the outcome of cross-coupling reactivity. That said, further investigations are needed to discern whether this trend stems from the dissociation of dinuclear species into mononuclear species, an association of mononuclear species into dinuclear ones, or similar reactivity of both.

■ CONCLUSIONS

This study advances the interface between CP synthesis and organometallic chemistry in several key ways. To begin, this work reports the first examples of Fe-catalyzed Kumada cross-coupling polymerizations of conjugated monomers in general as well as the use of diiron complexes in this context, specifically. We also establish reactivity trends for analogous mono- and dinuclear Fe and Ni complexes for both donor and acceptor CP synthesis. Substantial differences in polymerization reactivity are observed for Fe and Ni complexes—we observe step-growth for the former and chain-growth for the latter—with more subtle effects arising from complex nuclearity. Two dinuclear complexes in particular—**Fe_2—Cl_2^{2+}** and **Ni_2—Cl_2^{2+}**—stand out as "high performers" among their peers and present opportunities for further investigation in the context of cross-coupling. Additionally, we illuminate Csp^2—Csp^3 cross-coupling side-reactions that can, on the one hand complicate polymerization of conjugated monomers but, on the other, can enable the synthesis of novel nonconjugated materials. Although this work does not take a deeper dive into the polymerization mechanisms of individual precatalysts, the strategic focus on broad-stroke trend elucidation enabled us to explore a broad complex space, which we believe is most helpful at this stage to grow the young field of dinuclear catalysis for CP synthesis.

■ EXPERIMENTAL SECTION

Detailed synthetic procedures for monomers, precatalysts, and compounds used for cross-coupling reactions along with procedures and characterization data for polymerizations, cross-coupling reactions, and mechanistic studies of cross-coupling are covered in the Supporting Information.

Specifics for NMR spectroscopy, MALDI-TOF spectroscopy, GPC, high resolution mass spectrometry (HRMS), GC-MS, CV, elemental analysis, X-ray crystallography, UV—vis spectroscopy, and X-ray absorption spectroscopy are also contained in the Supporting Information.

General Procedure for Polymerization

To a vial equipped with a Teflon-coated stir bar was added 0.25 mL of a 3.0 mM solution of the precatalyst in anhydrous tetrahydrofuran (THF; to target 19:1 polymerizations) or 0.050 mL of a 3.0 mM solution of the precatalyst in anhydrous THF, which was diluted with 0.20 mL anhydrous THF (to target 95:1 polymerizations). To this solution was added 0.25 mL of a 60 mM stock solution of **BTZ** or

3HT. Polymerizations were quenched with 50 μL of a 1 M HCl solution prepared by the dilution of concentrated $HCl_{(aq)}$ with methanol after 6 h for ~19:1 polymerizations and after 24 h for ~95:1 polymerizations. Then, the conversion was analyzed by ^{1}H NMR spectroscopy in C_6D_6, followed by analysis using GPC-MALS to determine M_n, M_w, and $Đ$.

General Procedure for Cross-Coupling Reactions

To a 1-dram vial equipped with a Teflon-coated stir bar was added 0.90 mL of a stock solution with **Ar**−X (~33 mM) and **Ar**′−MgX. Then, 0.10 mL of a 14.9 mM solution of the precatalyst was added to give a 5% precatalyst loading. Reactions were stirred at RT and aliquots were quenched with proteomethanol; the solvent was removed under the flow of air, and the crude residue was dissolved in 0.5 mL of C_6D_6 for analysis with ^{1}H NMR spectroscopy.

ASSOCIATED CONTENT

Supporting Information

The Supporting Information is available free of charge at https://pubs.acs.org/doi/10.1021/acspolymersau.3c00022.

Materials and methods, synthetic and characterization procedures, supplementary text and figures, and spectral data (PDF)

Crystallographic data for **Fe_2−Br^+** (CCDC: 2289373) (CIF)

Crystallographic data for **PDI** (CCDC: 2289364) (CIF)

Crystallographic data for **Ni(PDI)Br_2** (CCDC: 2289372)(CIF)

Crystallographic data for **Fe(PDI)Cl_2** (CCDC: 2289363) (CIF)

Crystallographic data for **Ni(PDI)Br** (CCDC: 2289366) (CIF)

Crystallographic data for **Ni_2−Cl_2^{2+}** (CCDC: 2289365) (CIF)

AUTHOR INFORMATION

Corresponding Authors

Neil C. Tomson − *Department of Chemistry, University of Pennsylvania, Philadelphia, Pennsylvania 19104, United States*; orcid.org/0000-0001-9131-1039; Email: tomson@upenn.edu

Aleksandr V. Zhukhovitskiy − *Department of Chemistry, University of North Carolina at Chapel Hill, Chapel Hill, North Carolina 27514, United States*; orcid.org/0000-0002-3873-4179; Email: alexzhuk@email.unc.edu

Authors

Andrew J. King − *Department of Chemistry, University of North Carolina at Chapel Hill, Chapel Hill, North Carolina 27514, United States*

Jiashu Wang − *Department of Chemistry, University of Pennsylvania, Philadelphia, Pennsylvania 19104, United States*

Tianchang Liu − *Department of Chemistry, University of Pennsylvania, Philadelphia, Pennsylvania 19104, United States*; orcid.org/0000-0003-0629-6167

Adharsh Raghavan − *Department of Chemistry, University of Pennsylvania, Philadelphia, Pennsylvania 19104, United States*

Complete contact information is available at: https://pubs.acs.org/10.1021/acspolymersau.3c00022

Author Contributions

CRediT: **Andrew J King** conceptualization, data curation, formal analysis, investigation, methodology, writing-original draft, writing-review & editing; **Jiashu Wang** data curation, formal analysis, investigation, methodology, writing-review & editing; **Tianchang Liu** data curation, formal analysis, investigation, methodology, writing-review & editing; **Adharsh Raghavan** data curation, formal analysis, investigation, methodology, writing-review & editing; **Neil C. Tomson** conceptualization, data curation, formal analysis, funding acquisition, investigation, methodology, project administration, supervision, writing-original draft, writing-review & editing; **Aleksandr V. Zhukhovitskiy** conceptualization, data curation, formal analysis, funding acquisition, investigation, methodology, project administration, resources, supervision, writing-original draft, writing-review & editing.

Notes

The authors declare no competing financial interest.

ACKNOWLEDGMENTS

This material is based on work supported by general start-up funds provided by the University of North Carolina, Chapel Hill and the UNC−CH Department of Chemistry, as well as the funding provided by the DOD DAF Air Force Office of Scientific Research (AFOSR) Young Investigator Program (FA9550-23-1-0083) and the National Science Foundation under Grant no. 1945265. Instrumentation utilized for data collection in this work was supported by the AFOSR under grant FA9550-23-1-0077 (MALDI-TOF instrument grant) and the National Science Foundation under Grant no. 1828183 (NMR instrument grant), Grant no. 0922858 (NMR instrument grant), Grant no. CHE-1726291 (mass spectrometry grant), Grant no. 0650456 (elemental analysis grant), and Grant no. 2117783 (XANES grant). A.J.K. is supported by the Eliel Fellowship from the UNC Department of Chemistry. A.V.Z. is also supported by the 3M Non-Tenured Faculty Award. Any opinions, findings, conclusions, or recommendations expressed in this material are those of the author(s) and do not necessarily reflect the views of the National Science Foundation, the Department of Defense, or 3M. We thank Prof. Jillian Dempsey's group at UNC−CH, especially Alexandria Bredar, for their assistance with CV data collection and analysis. We thank the UNC-CH Department of Chemistry NMR Core Laboratory for the use of their NMR spectrometers and Mass Spectrometry Core Laboratory, especially Dr. Brandi Ehrmann and Lazaro Toledo for the use of their MALDI-TOF and assistance with mass spectrometry analysis. We thank Ryan P. Murphy for assistance with XANES data collection.

REFERENCES

(1) Lu, H.; Li, X.; Lei, Q. Conjugated Conductive Polymer Materials and Its Applications: A Mini-Review. *Front. Chem.* **2021**, *9*, No. 732132.

(2) Babudri, F.; Farinola, G. M.; Naso, F. Synthesis of Conjugated Oligomers and Polymers: The Organometallic Way. *J. Mater. Chem.* **2004**, *14* (1), 11−34.

(3) Seo, K.-B.; Lee, I.-H.; Lee, J.; Choi, I.; Choi, T.-L. A Rational Design of Highly Controlled Suzuki−Miyaura Catalyst-Transfer Polycondensation for Precision Synthesis of Polythiophenes and Their Block Copolymers: Marriage of Palladacycle Precatalysts with MIDA-Boronates. *J. Am. Chem. Soc.* **2018**, *140* (12), 4335−4343.

(4) Lee, J.; Kim, H.; Park, H.; Kim, T.; Hwang, S.-H.; Seo, D.; Chung, T. D.; Choi, T.-L. Universal Suzuki−Miyaura Catalyst-Transfer Polymerization for Precision Synthesis of Strong Donor/Acceptor-Based Conjugated Polymers and Their Sequence Engineering. *J. Am. Chem. Soc.* **2021**, *143* (29), 11180−11190.
(5) Kim, H.; Lee, J.; Kim, T.; Cho, M.; Choi, T.-L. Precision Synthesis of Various Low-Bandgap Donor−Acceptor Alternating Conjugated Polymers via Living Suzuki−Miyaura Catalyst-Transfer Polymerization. *Angew. Chem., Int. Ed.* **2022**, *61* (31), No. e202205828.
(6) Guo, X.; Facchetti, A. The Journey of Conducting Polymers from Discovery to Application. *Nat. Mater.* **2020**, *19* (9), 922−928.
(7) Leone, A. K.; McNeil, A. J. Matchmaking in Catalyst-Transfer Polycondensation: Optimizing Catalysts Based on Mechanistic Insight. *Acc. Chem. Res.* **2016**, *49* (12), 2822−2831.
(8) Pollit, A. A.; Ye, S.; Seferos, D. S. Elucidating the Role of Catalyst Steric and Electronic Effects in Controlling the Synthesis of π-Conjugated Polymers. *Macromolecules* **2020**, *53* (1), 138−148.
(9) Doyle, M. P.; Duffy, R.; Ratnikov, M.; Zhou, L. Catalytic Carbene Insertion into C−H Bonds. *Chem. Rev.* **2010**, *110* (2), 704−724.
(10) Furuya, T.; Kamlet, A. S.; Ritter, T. Catalysis for Fluorination and Trifluoromethylation. *Nature* **2011**, *473* (7348), 470−477.
(11) Hoffman, B. M.; Lukoyanov, D.; Yang, Z.-Y.; Dean, D. R.; Seefeldt, L. C. Mechanism of Nitrogen Fixation by Nitrogenase: The Next Stage. *Chem. Rev.* **2014**, *114* (8), 4041−4062.
(12) Powers, I. G.; Andjaba, J. M.; Luo, X.; Mei, J.; Uyeda, C. Catalytic Azoarene Synthesis from Aryl Azides Enabled by a Dinuclear Ni Complex. *J. Am. Chem. Soc.* **2018**, *140* (11), 4110−4118.
(13) Magnin, G.; Clifton, J.; Schoenebeck, F. A General and Air-Tolerant Strategy to Conjugated Polymers within Seconds under Palladium(I) Dimer Catalysis. *Angew. Chem., Int. Ed.* **2019**, *58* (30), 10179−10183.
(14) Buenaflor, J.; Sommerville, P.; Qian, H.; Luscombe, C. Investigation of Bimetallic Nickel Catalysts in Catalyst-Transfer Polymerization of π-Conjugated Polymers. *Macromol. Chem. Phys.* **2020**, *221* (2), No. 1900363.
(15) Andjaba, J. M.; Rybak, C. J.; Wang, Z.; Ling, J.; Mei, J.; Uyeda, C. Catalytic Synthesis of Conjugated Azopolymers from Aromatic Diazides. *J. Am. Chem. Soc.* **2021**, *143* (10), 3975−3982.
(16) King, A. J.; Zhukhovitskiy, A. V. A Chain-Growth Mechanism for Conjugated Polymer Synthesis Facilitated by Dinuclear Complexes with Redox-Active Ligands. *Angew. Chem., Int. Ed.* **2022**, *61* (29), No. e202206044.
(17) Leone, A. K.; Goldberg, P. K.; McNeil, A. J. Ring-Walking in Catalyst-Transfer Polymerization. *J. Am. Chem. Soc.* **2018**, *140* (25), 7846−7850.
(18) Zhang, S.; Wang, Q.; Thierer, L. M.; Weberg, A. B.; Gau, M. R.; Carroll, P. J.; Tomson, N. C. Tuning Metal−Metal Interactions through Reversible Ligand Folding in a Series of Dinuclear Iron Complexes. *Inorg. Chem.* **2019**, *58* (18), 12234−12244.
(19) Wang, Q.; Zhang, S.; Cui, P.; Weberg, A. B.; Thierer, L. M.; Manor, B. C.; Gau, M. R.; Carroll, P. J.; Tomson, N. C. Interdependent Metal−Metal Bonding and Ligand Redox-Activity in a Series of Dinuclear Macrocyclic Complexes of Iron, Cobalt, and Nickel. *Inorg. Chem.* **2020**, *59* (7), 4200−4214.
(20) Zhang, S.; Cui, P.; Liu, T.; Wang, Q.; Longo, T. J.; Thierer, L. M.; Manor, B. C.; Gau, M. R.; Carroll, P. J.; Papaefthymiou, G. C.; Tomson, N. C. N−H Bond Formation at a Diiron Bridging Nitride. *Angew. Chem., Int. Ed.* **2020**, *59* (35), 15215−15219.
(21) Liu, T.; Gau, M. R.; Tomson, N. C. Mimicking the Constrained Geometry of a Nitrogen-Fixation Intermediate. *J. Am. Chem. Soc.* **2020**, *142* (18), 8142−8146.
(22) Wang, Q.; Brooks, S. H.; Liu, T.; Tomson, N. C. Tuning Metal−Metal Interactions for Cooperative Small Molecule Activation. *Chem. Commun.* **2021**, *57* (23), 2839−2853.
(23) Thierer, L. M.; Wang, Q.; Brooks, S. H.; Cui, P.; Qi, J.; Gau, M. R.; Manor, B. C.; Carroll, P. J.; Tomson, N. C. Pyridyldiimine Macrocyclic Ligands: Influences of Template Ion, Linker Length and Imine Substitution on Ligand Synthesis. Structure Redox Properties. *Polyhedron* **2021**, *198*, No. 115044.
(24) Liu, T.; Murphy, R. P.; Carroll, P. J.; Gau, M. R.; Tomson, N. C. C−C σ-Bond Oxidative Addition and Hydrofunctionalization by a Macrocycle-Supported Diiron Complex. *J. Am. Chem. Soc.* **2022**, *144* (31), 14037−14041.
(25) Thierer, L. M.; Brooks, S. H.; Weberg, A. B.; Cui, P.; Zhang, S.; Gau, M. R.; Manor, B. C.; Carroll, P. J.; Tomson, N. C. Macrocycle-Induced Modulation of Internuclear Interactions in Homobimetallic Complexes. *Inorg. Chem.* **2022**, *61* (16), 6263−6280.
(26) Mako, T. L.; Byers, J. A. Recent Advances in Iron-Catalysed Cross Coupling Reactions and Their Mechanistic Underpinning. *Inorg. Chem. Front.* **2016**, *3* (6), 766−790.
(27) Cheng, S.; Zhao, R.; Seferos, D. S. Precision Synthesis of Conjugated Polymers Using the Kumada Methodology. *Acc. Chem. Res.* **2021**, *54* (22), 4203−4214.
(28) Mohadjer Beromi, M.; Banerjee, G.; Brudvig, G. W.; Charboneau, D. J.; Hazari, N.; Lant, H. M. C.; Mercado, B. Q. Modifications to the Aryl Group of Dppf-Ligated Ni σ-Aryl Precatalysts: Impact on Speciation and Catalytic Activity in Suzuki−Miyaura Coupling Reactions. *Organometallics* **2018**, *37* (21), 3943−3955.
(29) Greaves, M. E.; Ronson, T. O.; Lloyd-Jones, G. C.; Maseras, F.; Sproules, S.; Nelson, D. J. Unexpected Nickel Complex Speciation Unlocks Alternative Pathways for the Reactions of Alkyl Halides with Dppf-Nickel(0). *ACS Catal.* **2020**, *10* (18), 10717−10725.
(30) Chernyshev, V. M.; Ananikov, V. P. Nickel and Palladium Catalysis: Stronger Demand than Ever. *ACS Catal.* **2022**, *12* (2), 1180−1200.
(31) Setiawan, D.; Kalescky, R.; Kraka, E.; Cremer, D. Direct Measure of Metal−Ligand Bonding Replacing the Tolman Electronic Parameter. *Inorg. Chem.* **2016**, *55* (5), 2332−2344.
(32) Odian, G. Step Polymerization. In *Principles of Polymerization*; John Wiley & Sons, Ltd, 2004; pp 39−197.
(33) Hiemenz, P.; Lodge, T. Chain-Growth Polymerization. In *Polymer Chemistry*; CRC Press, 2007; pp 77−116.
(34) Carothers, W. H. Polymers and Polyfunctionality. *Trans. Faraday Soc.* **1936**, *32*, 39.
(35) Bedford, R. B.; Hall, M. A.; Hodges, G. R.; Huwe, M.; Wilkinson, M. C. Simple Mixed Fe−Zn Catalysts for the Suzuki Couplings of Tetraarylborates with Benzyl Halides and 2-Halopyridines. *Chem. Commun.* **2009**, *42*, 6430−6432.
(36) Hatakeyama, T.; Hashimoto, T.; Kondo, Y.; Fujiwara, Y.; Seike, H.; Takaya, H.; Tamada, Y.; Ono, T.; Nakamura, M. Iron-Catalyzed Suzuki−Miyaura Coupling of Alkyl Halides. *J. Am. Chem. Soc.* **2010**, *132* (31), 10674−10676.
(37) Bedford, R. B.; Carter, E.; Cogswell, P. M.; Gower, N. J.; Haddow, M. F.; Harvey, J. N.; Murphy, D. M.; Neeve, E. C.; Nunn, J. Simplifying Iron−Phosphine Catalysts for Cross-Coupling Reactions. *Angew. Chem., Int. Ed.* **2013**, *52* (4), 1285−1288.
(38) Crockett, M. P.; Tyrol, C. C.; Wong, A. S.; Li, B.; Byers, J. A. Iron-Catalyzed Suzuki−Miyaura Cross-Coupling Reactions between Alkyl Halides and Unactivated Arylboronic Esters. *Org. Lett.* **2018**, *20* (17), 5233−5237.

https://doi.org/10.1021/acspolymersau.3c00022
ACS Polym. Au 2023, 3, 475−481